FINAL REPORT

INSTABILITIES IN FISSIONING PLASMAS AS APPLIED TO THE GAS-CORE NUCLEAR ROCKET ENGINE

Submitted to:

National Aeronautics and Space Administration
Washington, D.C. 20546

by

VERSAR INC.
6621 Electronic Drive
Springfield, Virginia 22151

Final Report Due June 3, 1973
Contract NASw-2378

48 pp

ABSTRACT

An analysis has been made of the compressional wave spectrum excited in a fissioning uranium plasma confined in a cavity such as a gas cored nuclear reactor. Computer results are presented that solve the fluid equations for this problem including the effects of spatial gradients, nonlinearities, and neutron density gradients in the reactor. Typically the asymptotic fluctuation level for the plasma pressure is of order 1%.

TABLE OF CONTENTS

1. INTRODUCTION

The objective of this study has been to analyze the role of spatial gradients on the nonlinear development of fission power density driven instabilities in uranium plasmas. The principal impetus for study of such uranium plasma reactors has derived from the concept of a high specific impulse nuclear gas-cored rocket engine.[1-5] However, fissioning plasma reactors may also lead to development of a new class of magnetohydrodynamic generators[6-10], and perhaps may even have application to the direct nuclear excitation of lasers.[11]

The equations describing a uranium plasma involve the coupling of the plasma "fluid" dynamics to the neutron transport and also to the radiation transport in the system[12]. In such a reactor, the plasma would be enclosed (or nearly enclosed) by a neutron moderator — which is important in that it returns the thermalized neutrons back to the plasma core — while radiation transport dominates the transport of energy within the plasma. The system of equations used in this analysis is set out in the next section.

The major application for the fissioning uranium plasma reactor (on which significant effort has been expended) is that of the gas-cored nuclear rocket engine shown below. In general, this system consists of a chamber in which a fissioning uranium plasma (at $\sim 5 \cdot 10^4$°K) is maintained in the central region and radiatively heats the propellant hydrogen gas which flows around the main core and is subsequently ejected from the rocket nozzle. The chamber is surrounded by a moderator which slows down the fission neutrons and returns them to the uranium core.

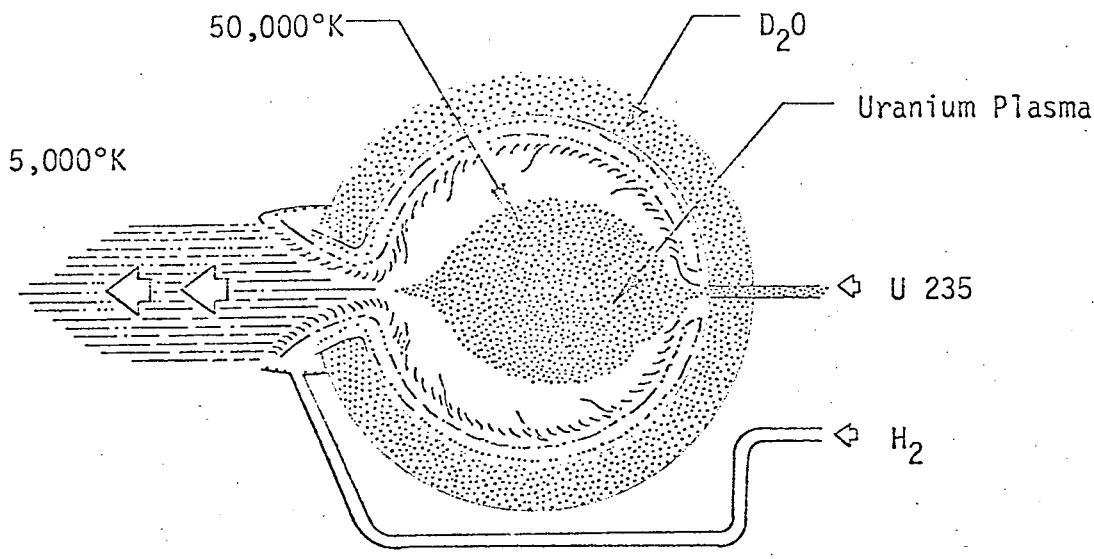

Figure 1.1

It is clear that if instabilities occur in this device, leading to either a fine-scale plasma turbulence or larger scale oscillations, they could well have undesirable results — such as enhancing the uranium fuel ejection from the rocket. An understanding of these processes (and their possible controllability) is of basic importance for the feasibility of constructing such plasma-cored rocket engines.

In a more general context, it should also be noted that the direct excitation of plasma motion and plasma waves by a fissioning plasma reactor may have useful applications to other energy conversion devices such as MHD generators.

One source of instability is the growth of sound waves[12] in the plasma due to the fission power density, P_{fiss}. The instability

mechanism involved can be understood as follows: Consider a standing sound wave in a bounded region of fissioning plasma with a constant background thermal neutron density. In the wave compressions the fission power density, P_{fiss}, increases due to the increased uranium density, and in the rarefactions P_{fiss} decreases. This results in an increased pressure gradient associated with the wave which in turn leads to a transfer of fission power to the wave. It occurs because the wave compression tends to expand more rapidly than it was compressed. However, competing with this is the fact that radiation tends to transport the extra thermal energy out of the wave compressions. Radiation diffusion smooths out the temperature fluctuations of waves more rapidly the shorter their wavelength. This results in a critical wavelength, λ_{crit}, below which waves are stable and above which they are unstable.

Last year we calculated the nonlinear evolution of such unstable waves to determine their limiting amplitude. The mechanism that finally limits their amplitude is the mode coupling of unstable waves in the wavelength range $\lambda > \lambda_{crit}$ to radiation damped waves in the range $\lambda < \lambda_{crit}$. However in order to keep the equations tractable it was assumed that the uranium plasma was spatially homogeneous, and that only one mode was unstable.

The work reported here relaxes these assumptions and deals with the full system of equations including the physical effects of nonuniform plasma density, temperature, neutron density, and radiation flux, on acoustic instabilities in the reactor. The temperature dependence of the Rosseland diffusion coefficient and internal ionization energy storage in the plasma

was also included.

The system of fluid equations describing a U-plasma heated by fission and losing energy by radiation diffusion is given by Eqs. (2.1)-(2.3) in the next section. Our procedure is to first choose a stationary solution to these equations corresponding to a given steady-state reactor. Then, a computer solution is obtained which follows the evolution of a perturbation in the plasma.

Our general conclusion is that for typical parameters (of interest for gas core rocket engines), the pressure fluctuation level due to fission-driven acoustic instabilities is of order 1%. The fact that this is considerably larger than that calculated last year can be assigned to the capability of the computer model to include the effects of spatial inhomogeneities for a reactor in which several modes are also unstable. These complex situations could not be treated by analytic methods.

The above fluctuation level should not present a severe problem for open cycle reactors. Further, under some conditions (see section 5), the partial transmission of sound waves out of the reactor cavity would have an important stabilizing effect which could suppress the fluctuations to below the 1% level. In an open cycle reactor, acoustic compression waves can propagate out of the cavity along the gas column ejected through the rocket nozzle (and a small amount of transmission can also occur through the walls). This competes with the fission power density effect that tends to energize such waves.

2. FLUID EQUATIONS FOR URANIUM PLASMA

It is useful for computational purposes to write the system of fluid equations for a U-plasma in conservation law form. We start with[12],

$$\frac{\partial N_u}{\partial t} + \underline{\nabla} \cdot (N_u \underline{V}_u) = 0 \tag{2.1}$$

$$\frac{\partial \underline{V}_u}{\partial t} + \underline{V}_u \cdot \underline{\nabla}\, \underline{V}_u + \frac{1}{M N_u} \underline{\nabla} \left[N_u K T_u (1 + Z)\right] = 0 \tag{2.2}$$

$$\left(\frac{\partial}{\partial t} + \underline{V}_u \cdot \underline{\nabla}\right) \left[\frac{3}{2} N_u K T_u (1 + Z) + N_u \mathcal{E}\right] + \frac{5}{2} (1 + Z)\, N_u K T_u \underline{\nabla} \cdot \underline{V}_u$$

$$+ N_u \mathcal{E}\, \underline{\nabla} \cdot \underline{V}_u = P_{fiss} + \underline{\nabla} \cdot \left[K_R \underline{\nabla} T_u\right] \quad . \tag{2.3}$$

where the fission power density, P_{fiss}, is given by

$$P_{fiss} = N_u N_n v_o \sigma Q$$

and

N_u = number density of U atoms and ions

V_u = radial fluid velocity

Z = mean charge on U atoms or ions in units of e

M = mass of U-atom

T_u = U-plasma temperature

N_n = neutron number density

v_o = neutron thermal speed

Q = energy per fission event

σ = induced fission cross-section

K_R = radiation diffusion coef. ($\equiv$ a thermal conductivity)

$\mathcal{E}$ = average energy used to ionize the U atoms to their average charge state Z

The quantities $\mathcal{E}$ and Z are shown[12-16] as functions of T and pressure in figures 2.1 and 2.2.

The last two equations can be re-written

$$\frac{\partial}{\partial t}\left(MN_u\underline{V}_u\right) + \underline{\nabla}\cdot\left[MN_u\underline{V}_u\underline{V}_u + \underline{\underline{I}}\,N_uKT_u\,(1+Z)\right] = 0 \qquad (2.4)$$

$$\frac{\partial}{\partial t}\left\{\frac{1}{2}MN_uV_u^2 + \frac{3}{2}N_uKT_u(1+Z) + N_u\mathcal{E}\right\} ,$$

$$+\underline{\nabla}\cdot\left\{\underline{V}_u\,\frac{1}{2}MN_uV_u^2 + \frac{5}{2}\underline{V}_uN_uKT_u(1+Z) + N_u\underline{V}_u\mathcal{E} - K_R\underline{\nabla}T_u\right\} = P_{fiss}, \qquad (2.5)$$

thereby expressing their local conservation-law form.

Considering for example the motion of a plasma confined to a slab of thickness L with rigid walls, *i.e.*,

$$V_u(x = 0,L) = 0 ,$$

the instantaneous heat flux out of the reactor is

$$P_{Tot} = -K_R\left(\frac{\partial T_u}{\partial x}\right)_{x=0,L} \text{ ergs/sec/cm}^2 .$$

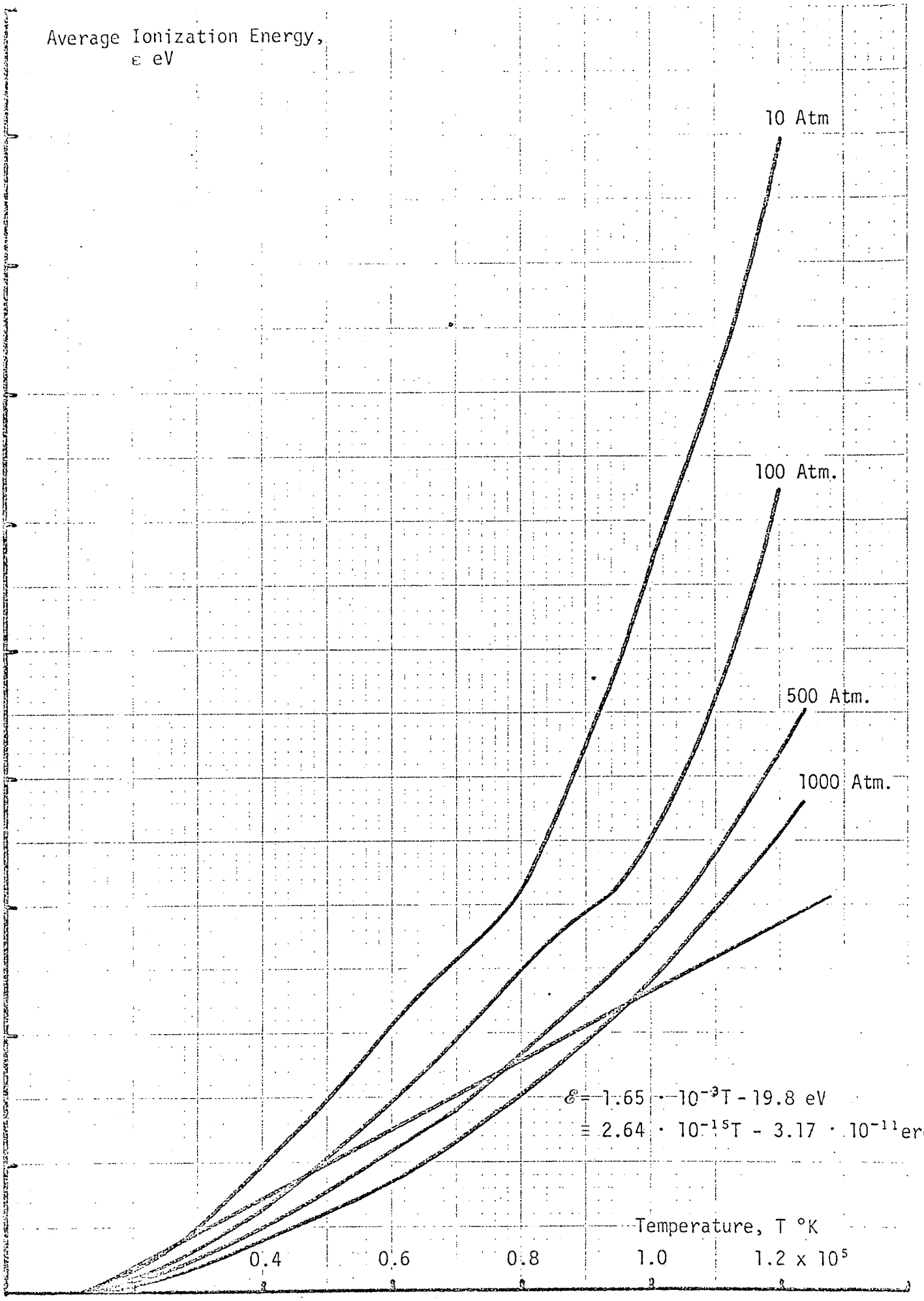
Average Ionization Energy,
ε eV
560
540
480
420
360
300
240
180
120
60
10 Atm
100 Atm.
500 Atm.
1000 Atm.
$\mathcal{E} = 1.65 \cdot 10^{-3}T - 19.8$ eV
$= 2.64 \cdot 10^{-15}T - 3.17 \cdot 10^{-11}$ ergs
Temperature, T °K
0.4
0.6
0.8
1.0
1.2 x 10⁵

Figure 2.1

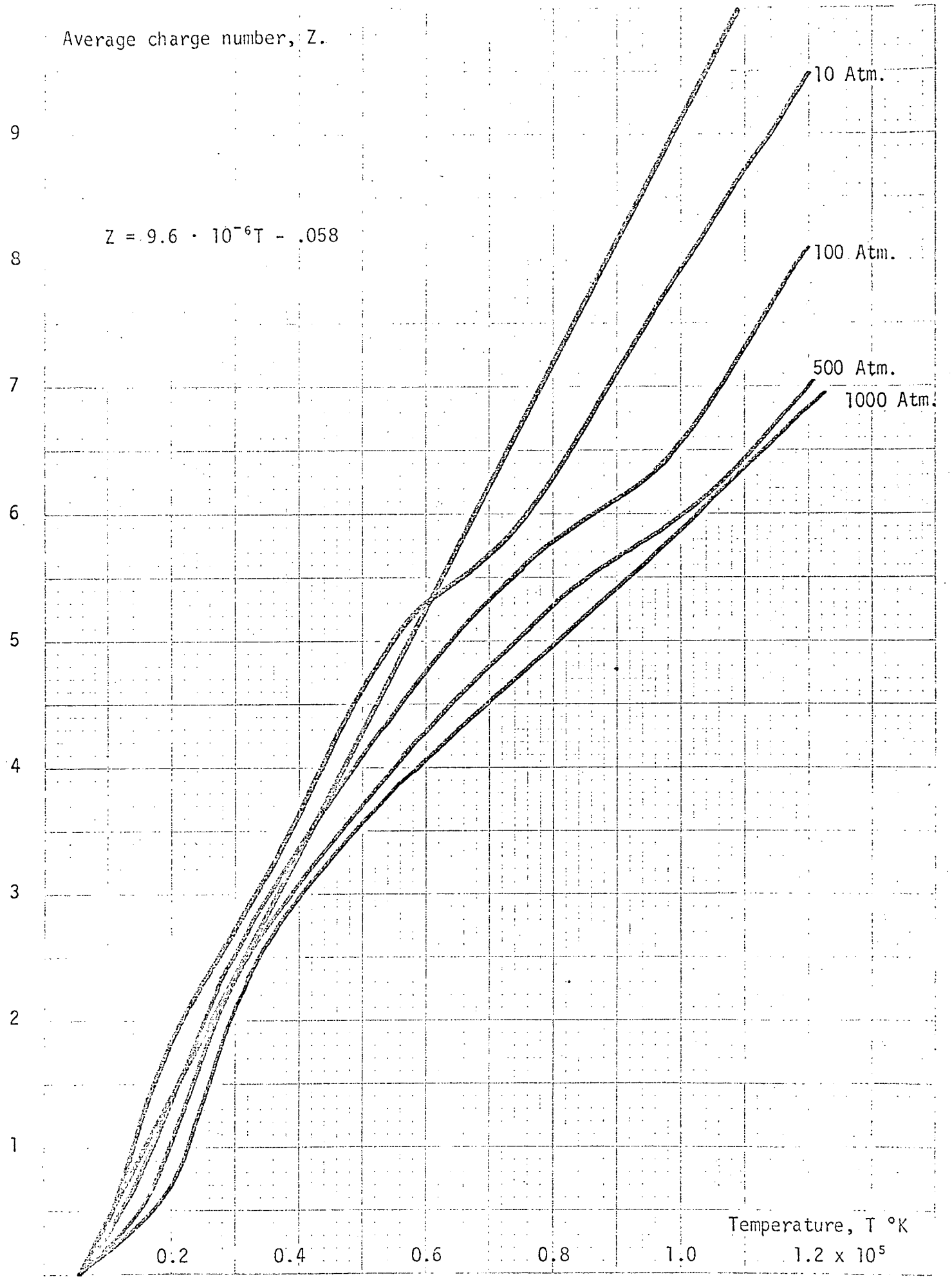
Average charge number, Z.
$Z = 9.6 \cdot 10^{-6}T - .058$
10 Atm.
100 Atm.
500 Atm.
1000 Atm.
9
8
7
6
5
4
3
2
1
0.2
0.4
0.6
0.8
1.0
1.2 x 10^5
Temperature, T °K

Figure 2.2

This is a radiation flux and is assumed to be carried off at the outer wall by for example a flow of cooler absorbing fluid. We will be interested in an initial value problem in which the system starts at t = 0 with small perturbation about a steady state solution. A spectrum of waves is then expected to be generated which reaches a steady-spectrum state.

Equations in Dimensionless Form

The following dimensionless variables are useful:

$$\underline{X} = \frac{x}{L}$$

$$\tau = t/(L/V_o) \tag{2.6}$$

where L is a length in the system (*e.g.*, sphere radius or slab thickness), and

$$V_o = \left[\frac{KT_o(1 + Z_o)}{M}\right]^{\frac{1}{2}} = \left(\frac{P_o}{\rho_o}\right)^{\frac{1}{2}}$$

where P_o, ρ_o, T_o, Z_o, N_o, are all evaluated at the central point in the system. Thus we define

$$\begin{cases} \rho = \left(\dfrac{MN_u}{MN_o}\right) \\ T = \dfrac{T_u}{T_o} \\ V = \dfrac{V_u}{V_o} \end{cases} \tag{2.7}$$

Further, define

$$\begin{cases} \theta = \dfrac{1 + Z}{1 + Z_o} \\ \\ \varepsilon = \dfrac{\mathcal{E}}{KT_o(1 + Z_o)} \end{cases} \qquad (2.8)$$

In terms of these variables the system becomes

$$\frac{\partial}{\partial \tau} \begin{pmatrix} \rho \\ \rho \underline{V} \\ \frac{1}{2} \rho V^2 + \frac{3}{2} \rho T\theta + \rho\varepsilon \end{pmatrix} + \frac{\partial}{\partial \underline{X}} \cdot \begin{pmatrix} \rho \underline{V} \\ \rho \underline{V}\underline{V} + \underline{\underline{I}} \rho T\theta \\ \frac{1}{2} \rho V^2 \underline{V} + \frac{5}{2} \underline{V} \rho T\theta + \rho \underline{V}\varepsilon - \dfrac{K_R T_o}{\rho_o V_o^3 L} \dfrac{\partial T}{\partial \underline{X}} \end{pmatrix}$$

$$= \begin{pmatrix} 0 \\ 0 \\ L P_{fiss}/\rho_o V_o^3 \end{pmatrix} . \qquad (2.9)$$

The dependence of the radiation diffusion coefficient and fission power density on T, N is given below.

Radiation Diffusion Coefficient[12-16]

The radiation diffusion coefficient is given by

$$K_R = \frac{16}{3} \frac{\sigma_B T_u^3}{k_R} \qquad (2.10)$$

where σ is the black body constant and k_R the Rosseland mean opacity in cm^{-1}.

Now there is some uncertainty concerning the T_u and pressure dependence of k_R. Some theoretical values are shown below, which according to Patch are expected to be correct to within an order of magnitude. Typically we shall be interested in the temperature range from 50,000 °K (reactor core) to 5000 °K (reactor edge). In this range we see that k_R goes through a maximum. In view of uncertainties in the value of k_R, and the fact that the T^3 dependence in (2.10) is stronger than the $k_R(T)$ dependence, we shall simply assume k_R to be constant in the following calculations. It would not be difficult to relax this assumption.

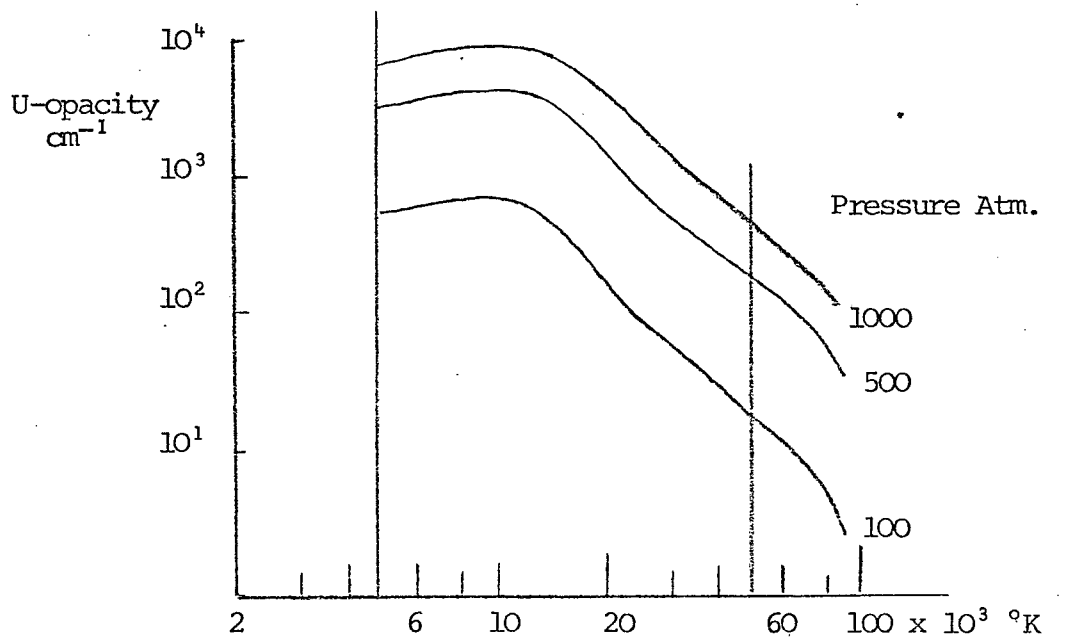

Figure 2.3

The quantity occurring in the dimensionless equation (2.9) involving radiation diffusion has a coefficient

$$\frac{K_R T_o}{\rho_o V_o^3 L} = \frac{16 \sigma_B T_o^3}{3 k_R}\left(\frac{T_o}{\rho_o V_o^3 L}\right) T^3 \equiv \bar{K}_R T^3 \tag{2.11}$$

where we have defined a dimensionless diffusion coefficient $\bar{K}_R$. This can also be written

$$\bar{K}_R = K_{Ro}\left(\frac{T_o}{L\rho_o V_o^3}\right) = \frac{K_{Ro}}{V_o N_o K(1+Z)L} \tag{2.12}$$

where K_{Ro} is K_R evaluated at the reference point x_o where $T_u = T_o$, $N_u = N_o$.

Fission Power Density

The dimensionless quantity involving fission in (2.9) is

$$\left(\frac{L}{\rho_o V_o^3}\right) P_{fiss} = \left(\frac{L}{\rho_o V_o^3}\right) N_u N_n v_o \sigma Q \ .$$

For the neutron density in the cavity we allow a space dependence and write

$$N_n = \eta_n g(X)$$

where $g(X_o) = 1$ evaluated at the reference point x_o. Thus,

$$\left(\frac{L}{\rho_o V_o^3}\right) P_{fiss} \equiv \overline{P}_{fiss}\ \rho\ g(X) \tag{2.13}$$

where the dimensionless fission power is

$$\overline{P}_{fiss} = \frac{L}{\rho_o V_o^3} P_{fiss,o} = \frac{v_o \sigma Q R \eta_n}{K T_o (1 + Z_o) V_o} \tag{2.14}$$

and

$$P_{fiss,o} = N_o \eta_n v_o \sigma Q \tag{2.15}$$

is the fission power at the central point x_o where $N_u = N_o$ and $T_u = T_o$.

Equations for Slab or Sphere

In summary then, equation (2.9) can be written as

$$\frac{\partial}{\partial \tau}\begin{pmatrix} \rho \\ \rho \underline{V} \\ \frac{1}{2}\rho V^2 + \frac{3}{2}\rho T\theta + \rho\varepsilon \end{pmatrix} + \frac{\partial}{\partial \underline{X}} \cdot \begin{pmatrix} \rho \underline{V} \\ \rho \underline{V}\,\underline{V} + \underline{\underline{I}}\,\rho T\theta \\ \frac{1}{2}\rho V^2 \underline{V} + \frac{5}{2}\underline{V}\rho T\theta + \rho \underline{V}\varepsilon - \overline{K}_R T^3 \frac{\partial T}{\partial \underline{X}} \end{pmatrix}$$

$$= \begin{pmatrix} 0 \\ 0 \\ \overline{P}_{fiss}\ \rho g(X) \end{pmatrix} . \tag{2.16}$$

This equation is simplest to integrate for one-dimensional geometries

such as slabs, spheres, or cylinders. It becomes complicated for two dimensions, and only a few 3-D fluid codes have been written to date and invariably consume large quantities of machine time or the use of extremely coarse grids. Two one-dimensional cases of interest to us are:

Slab

$$\frac{\partial}{\partial \tau}\begin{pmatrix} \rho \\ \rho V \\ \frac{1}{2}\rho V^2 + \frac{3}{2}\rho T\theta + \rho\varepsilon \end{pmatrix} + \frac{\partial}{\partial X}\begin{pmatrix} \rho V \\ \rho V^2 + \rho T\theta \\ \frac{1}{2}\rho V^3 + \frac{5}{2} V\rho T\theta + \rho V\varepsilon - \bar{K}_R T^3 \frac{\partial T}{\partial X} \end{pmatrix} \tag{2.16a}$$

$$= \begin{pmatrix} 0 \\ 0 \\ \bar{P}_{fiss}\, \rho\, g \end{pmatrix} .$$

Sphere

$$\frac{\partial}{\partial \tau}\begin{pmatrix} R^2\rho \\ \rho V \\ R^2\left[\frac{1}{2}\rho V^2 + \frac{3}{2}\rho T\theta + \rho\varepsilon\right] \end{pmatrix} + \frac{\partial}{\partial \tau}\begin{pmatrix} R^2\rho V \\ \rho V^2 + \rho T\theta \\ R^2\left[\frac{1}{2}\rho V^3 + \frac{5}{2} V\rho T\theta + \rho V\varepsilon - \bar{K}_R T^3 \frac{\partial T}{\partial R}\right] \end{pmatrix} \tag{2.16b}$$

$$= \begin{pmatrix} 0 \\ 0 \\ R^2 P_{fiss}\, \rho\, g \end{pmatrix} .$$

It should be noted that the quantities Z and $\mathcal{E}$ are also functions of T and P. They occur in (2.16) in the dimensionless variables

$$\theta = \frac{1 + Z}{1 + Z_0} \quad , \epsilon = \frac{\mathcal{E}}{KT_o(1 + Z_o)} \quad . \tag{2.17}$$

Now the temperature dependence of Z, $\mathcal{E}$ is more rapid than their pressure dependence. Also, the reactor plasma will have a pressure which is nearly constant as a function of position (except for fluctuations associated with wave motion), whereas the plasma temperature varies by an order of magnitude from the center of the reactor edge. Thus it is reasonable to set

$$\begin{aligned} Z(T, P) &\cong Z(T, P_o) \\ \mathcal{E}(T, P) &\cong \mathcal{E}(T, P_o) \end{aligned} \tag{2.18}$$

in the fluid equations, i.e., only account for the temperature dependence of Z, $\mathcal{E}$ in the time-dependent problem.

This has been done by making a linear fit of the UPLAZ-2 computer calculations[4] for these functions, i.e.,

$$\begin{aligned} Z &= a + b\, T_u \equiv a + b\, T_o\, T \\ \mathcal{E} &= c + d\, T_u \equiv c + d\, T_o\, T \quad . \end{aligned} \tag{2.19}$$

The coefficients a, b, c, d are functions of pressure evaluated at the approximately constant reactor pressure.

3. STATIONARY SOLUTIONS

From equation (2.16) we see that the stationary solutions involve solving

$$\rho T\Theta = 1 \tag{3.1}$$

and

$$\overline{K}_R \frac{\partial}{\partial X}\left(T^3 \frac{\partial T}{\partial X}\right) + \overline{P}_{fiss}\,\rho\, g(X) = 0 \qquad \text{(slab)} \tag{3.2}$$

or

$$\overline{K}_R \frac{\partial}{\partial R}\left(T^3R^2 \frac{\partial T}{\partial R}\right) + \overline{P}_{fiss}\,\rho\, g(R)R^2 = 0 \qquad \text{(sphere)}\ . \tag{3.3}$$

Using (3.1), these become

$$(1 + Z)T \frac{\partial}{\partial X}\left(T^3\frac{\partial T}{\partial X}\right) + \xi\, g(X) = 0 \qquad \text{(slab)} \tag{3.4}$$

$$(1 + Z)T \frac{\partial}{\partial R}\left(T^3R^2\frac{\partial T}{\partial R}\right) + \xi R^2 g(R) = 0 \qquad \text{(sphere)} \tag{3.5}$$

where

$$\xi = \frac{\overline{P}_{fiss}(1 + Z_o)}{\overline{K}_R}$$

i.e.,

$$3\left(\frac{\partial T}{\partial R}\right)^2 + T\frac{\partial^2 T}{\partial X^2} + \frac{\xi\, g}{(1 + Z)T^3} = 0 \qquad \text{(slab)} \tag{3.6}$$

$$3\left(\frac{\partial T}{\partial R}\right)^2 + T\frac{\partial^2 T}{\partial R^2} + \frac{2T}{R}\frac{\partial T}{\partial R} + \frac{\xi\, g}{(1 + Z)\,T^3} = 0 \qquad \text{(sphere)} \tag{3.7}$$

Now writing the grid spacing as h, it follows that

$$\left.\frac{\partial T}{\partial X}\right|_{atj} \simeq \frac{1}{2h}\ (T_{j+1} - T_{j-1})$$

$$\left.\frac{\partial^2 T}{\partial X^2}\right|_{j} \simeq \frac{1}{h^2}\ (T_{j+1} - 2T_j + T_{j-1}) \qquad (3.8)$$

$$\left(\frac{\partial T}{\partial X}\right)^2 \simeq \frac{1}{4h^2}\ (T^2_{j+1} - 2T_{j+1}\,T_{j-1} + T^2_{j-1})\ .$$

Thus (3.6) or (3.7) give a quadratic in T_{j+1} :

$$A\,T^2_{j+1} + B\,T_{j+1} + C = 0$$

$$T_{j+1} = \frac{1}{2A}\left(-B + (B^2 - 4AC)^{\frac{1}{2}}\right) \qquad (3.9)$$

where

slab

$$\begin{cases} A = \dfrac{3}{4} \\ B = T_j - \dfrac{3}{2}\,T_{j-1} \\ C = \dfrac{3}{4}\,T^2_{j-1} - 2T^2_j + T_jT_{j-1} + \dfrac{\xi\,h^2 g(X = jh)}{T^3_j(1 + a + bT_oT_j)} \end{cases} \qquad (3.10)$$

Sphere

$$\begin{cases} A = \dfrac{3}{4} \\ B = T_j - \dfrac{3}{2}\,T_{j-1} + \dfrac{hT_j}{R_j} \\ C = \dfrac{3}{4}\,T^2_{j-1} - 2T^2_j + T_jT_{j-1} - \dfrac{h}{R_j}\,T_jT_{j-1} + \dfrac{\xi\,h^2 g(R_j)}{T^3_j(1 + a + bT_oT_j)} \end{cases} \qquad (3.11)$$

where we have noted equation (2.19) for Z .

Some sample curves are shown in Figs. 3.1 to 3.4 for a slab of thickness L (L is taken as the reference length in Eq. 2.6). The reference point where $N_u = N_o$, $T_u = T_o$ is taken as the center, i.e., x = L/2, X = .5, and the neutron density function g was taken to be

$$g = e^{\alpha(x - \frac{L}{2})^2} \equiv e^{\alpha L^2 (X - .5)^2} .$$

The constants used in Figs. 3.1 - 3.4 are:

$$\begin{cases} \left.\begin{aligned} a &= -.4375 \\ b &= 9.37 \cdot 10^{-5} \end{aligned}\right\} \quad \text{for } Z = a + bT_oT \\ Z_o = 4.247 \\ T_o = 5 \cdot 10^4 \ ^\circ K \\ \alpha L^2 = 2 \text{ or } 0 \qquad \text{(Scale for neutron density)} \\ N_o = 1.5\ 10^{19} \\ k_R = 1.2\ 10^2\ cm^{-1} \\ \left.\begin{aligned} c &= -3.17 \cdot 10^{-11} \\ e &= 2.64 \cdot 10^{-15} \end{aligned}\right\} \quad \text{for } \xi = c + dT_oT \\ \text{Various values of } \xi \text{ which determines } P_{fiss,o} \cdot \\ K_{Ro} = 3.2 \cdot 10^8 \text{ erg/sec/deg.} \end{cases} \qquad (3.12)$$

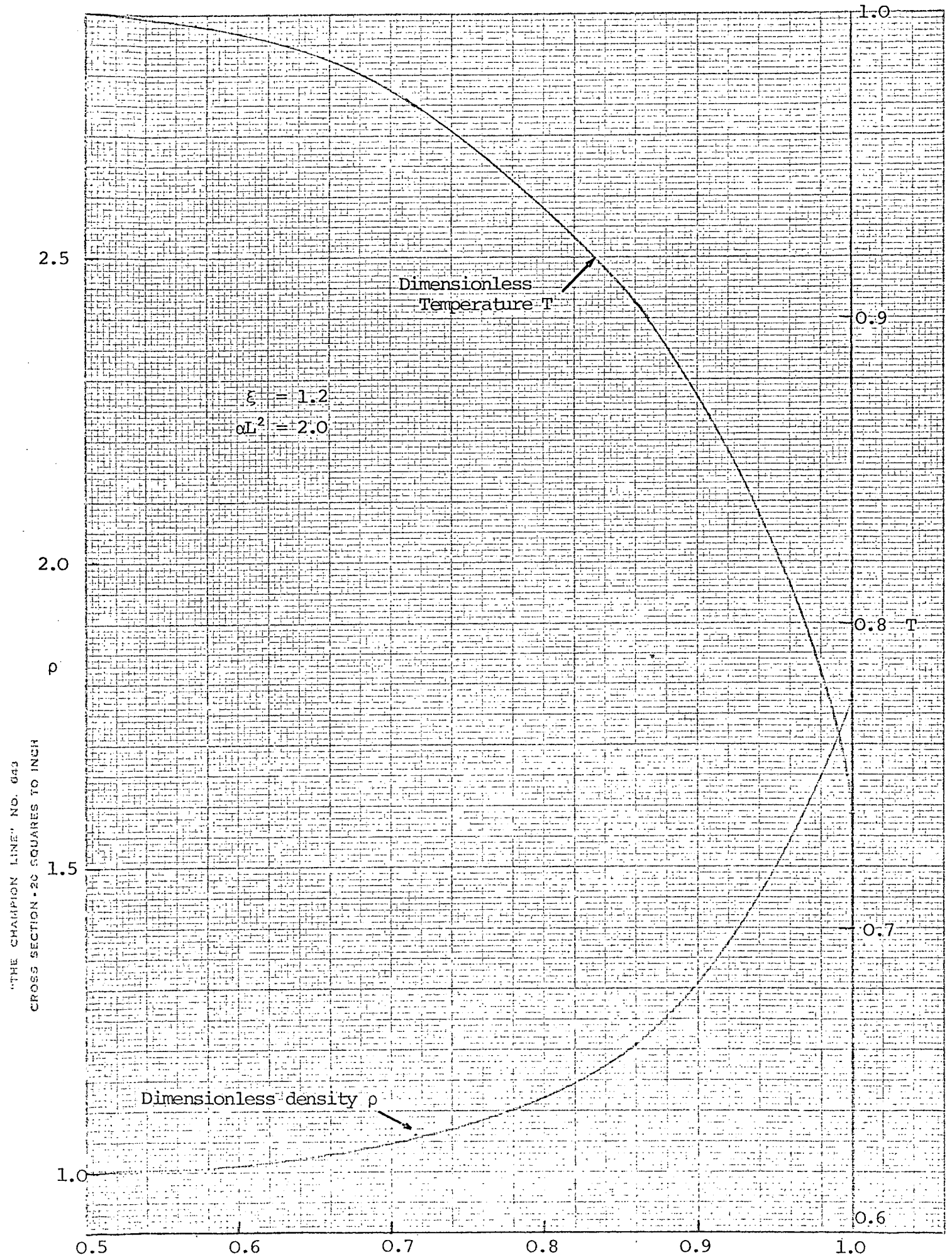
Dimensionless Temperature T
$\xi = 1.2$
$\alpha L^2 = 2.0$
Dimensionless density ρ
ρ
T
X = x/L
2.5
2.0
1.5
1.0
0.9
0.8
0.7
0.6
0.5
0.6
0.7
0.8
0.9
1.0
"THE CHAMPION LINE" NO. 643
CROSS SECTION - 20 SQUARES TO INCH

Figure 3.1

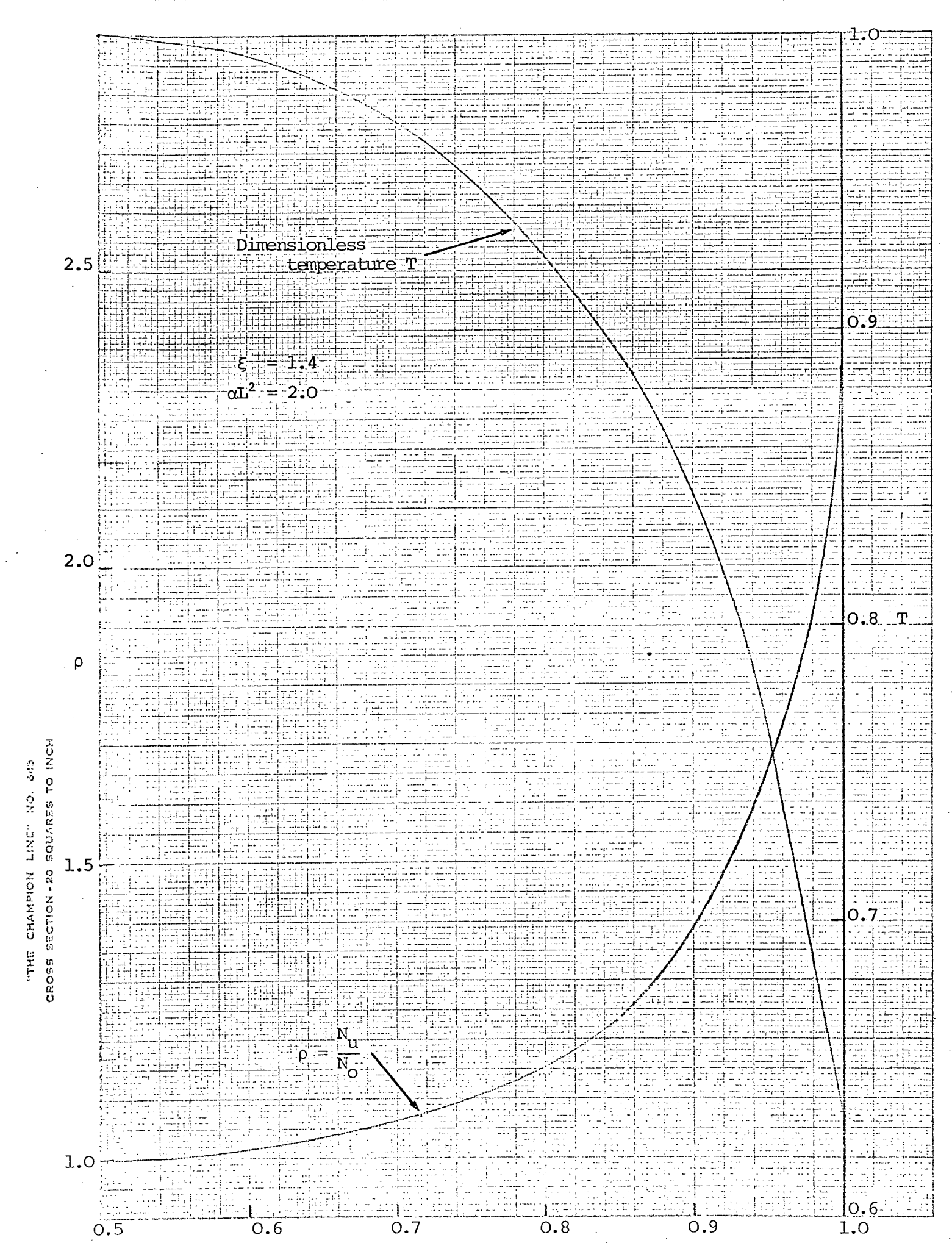
Dimensionless
temperature T
$\xi = 1.4$
$\alpha L^2 = 2.0$
$\rho = \frac{N_u}{N_o}$
ρ
T
X = x/L
2.5
2.0
1.5
1.0
0.9
0.8
0.7
0.6
0.5
0.6
0.7
0.8
0.9
1.0
"THE CHAMPION LINE" NO. 643
CROSS SECTION - 20 SQUARES TO INCH

Figure 3.2

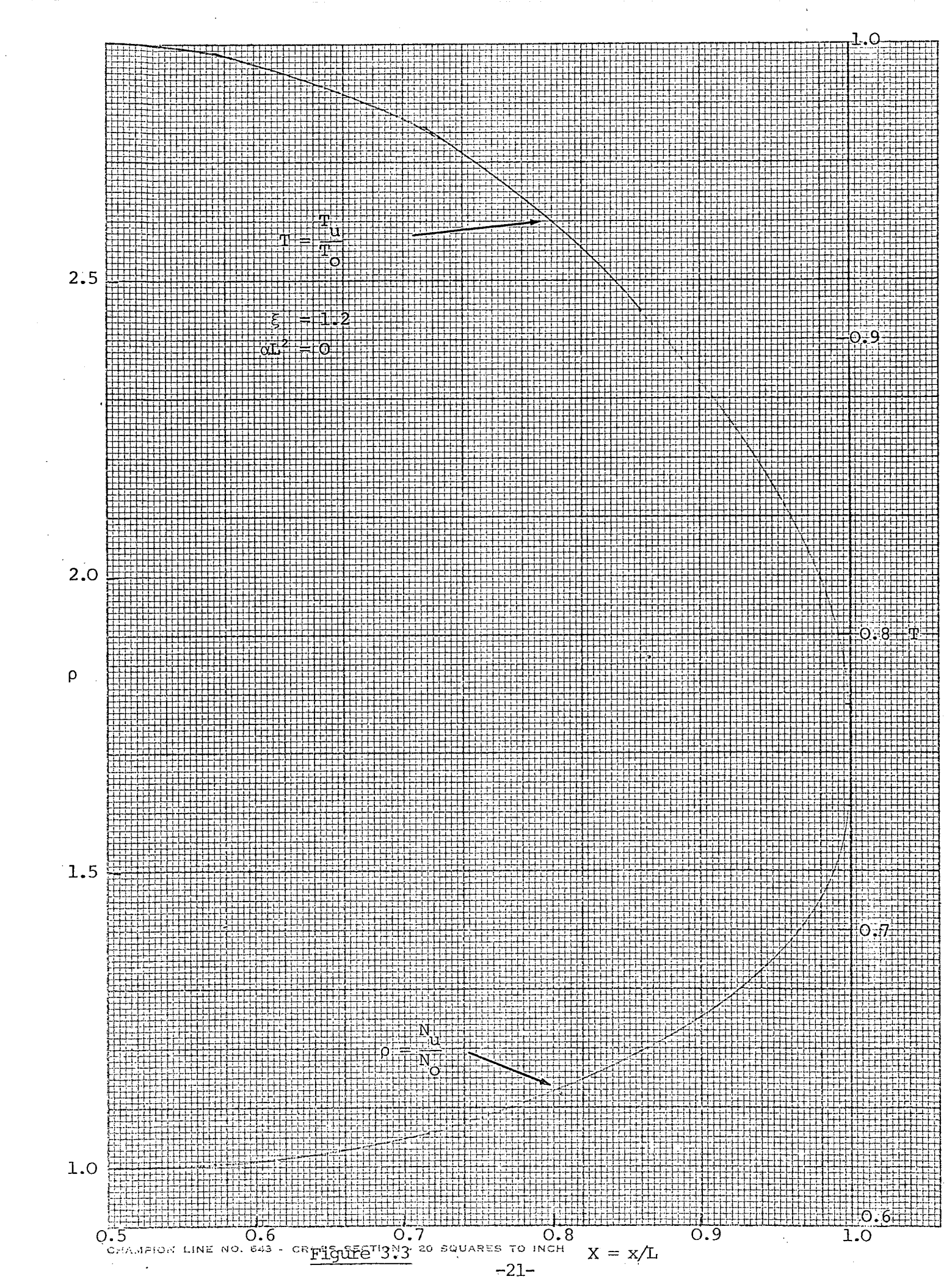
1.0
2.5
2.0
1.5
1.0
ρ
$T = \frac{T_u}{T_o}$
$\xi = 1.2$
$\alpha L^2 = 0$
0.9
0.8
T
0.7
0.6
$\rho = \frac{N_u}{N_o}$
0.5
0.6
0.7
0.8
0.9
1.0
X = x/L
CHAMPION LINE NO. 643 - CROSS SECTION 20 SQUARES TO INCH

Figure 3.3

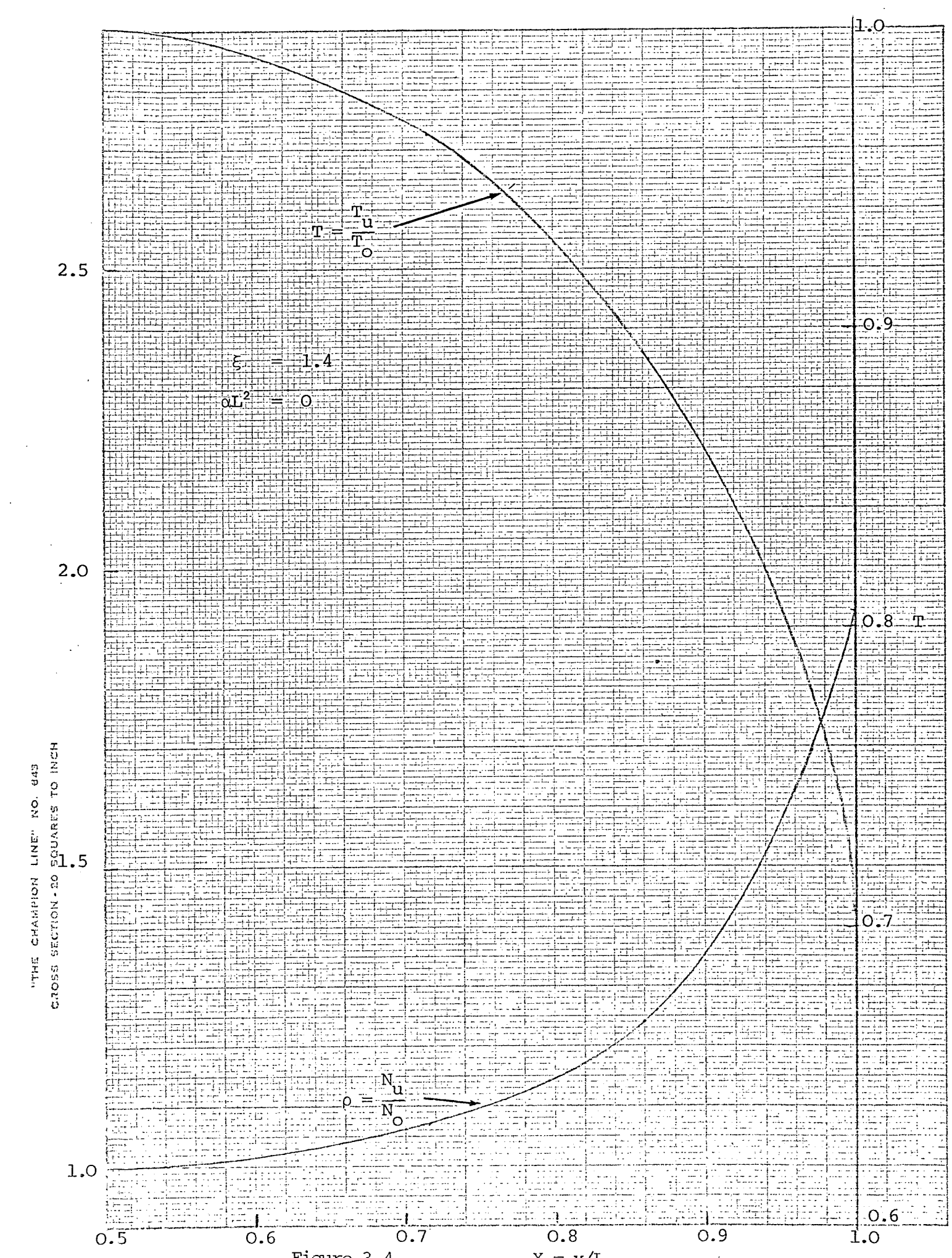
$T = \frac{T_u}{T_o}$
$\xi = 1.4$
$\alpha L^2 = 0$
$\rho = \frac{N_u}{N_o}$
T
2.5
2.0
1.5
1.0
0.9
0.8
0.7
0.6
0.5
0.6
0.7
0.8
0.9
1.0
X = x/L
"THE CHAMPION LINE" NO. 643
CROSS SECTION - 20 SQUARES TO INCH

Figure 3.4

4. TIME-DEPENDENT PROBLEM

The program that integrates (2.16a) makes use of the Lax Wendrof two step method. Equation (2.16a) has the form

$$\frac{\partial}{\partial \tau} \underline{u} + \frac{\partial}{\partial x} \underline{F} = \underline{D} \quad . \tag{4.1}$$

Step 1:

Compute provisional values at centers of rectangular meshes of the net in the $x - \tau$ plane using

$$\underline{U}_{j+\frac{1}{2}}^{n+\frac{1}{2}} = \frac{1}{2} (\underline{U}_{j+1}^{n} + \underline{U}_{j}^{n}) - \frac{\Delta\tau}{2\Delta x} (\underline{F}_{j+1}^{n} - \underline{F}_{j}^{n}) + \frac{\Delta\tau}{4} (\underline{D}_{j+1}^{n} + \underline{D}_{j}^{n}) \quad . \tag{4.2}$$

Step 2:

Then advance in time using

$$\underline{U}_{j}^{n+1} = \underline{U}_{j}^{n} - \frac{\Delta\tau}{\Delta x} (\underline{F}_{j+\frac{1}{2}}^{n+\frac{1}{2}} - \underline{F}_{j-\frac{1}{2}}^{n+\frac{1}{2}}) + \frac{\Delta\tau}{2} (D_{j+\frac{1}{2}} + \underline{D}_{j-\frac{1}{2}}) . \tag{4.3}$$

The walls are treated as rigid so that the fluid flux ρV vanishes there. However, the energy flux is a floating quantity at the wall, i.e., it is continuous across the boundary. A spatial Fourier analysis is also made of the various fluid variables,

$$\begin{aligned} A &= \Sigma \ (A_n \sin k_n x + B_n \cos k_n x) \\ k_n &= \frac{\pi n}{L} \end{aligned} \tag{4.4}$$

Interpretation of Fourier Mode Behavior and Comments on Turbulence Equations

When the stationary system described in Section 3 is perturbed, a spectrum of sound waves is generated. This spectrum settles down into an asymptotic finite amplitude spectrum after about 50 sound transit times across the reactor. It derives its energy from the fission power driven instability described earlier.[12]

Now the presence of such a wave spectrum also causes the time-average temperature and density profiles across the reactor (about which fluctuations occur) to depart from the steady state solutions of section 3. One can clarify this as follows:

First define a time average over a time scale larger than the wave periods,

$$\langle\ \rangle = \frac{1}{T} \int_{-T/2}^{T/2} dt \tag{4.5}$$

with $T >> \omega_n^{-1}$. The averaged fluid equations (2.16) then become

$$\frac{\partial}{\partial T} \left\langle \begin{pmatrix} \rho \\ \rho \underline{V} \\ \frac{1}{2}\rho V^2 + \frac{3}{2}\rho T\Theta + \rho\varepsilon \end{pmatrix} \right\rangle + \frac{\partial}{\partial \underline{X}} \cdot \left\langle \begin{pmatrix} \rho \underline{V} \\ \rho \underline{V}\underline{V} + \underline{\underline{I}}\rho T\Theta \\ \frac{1}{2}\rho V^2 \underline{V} + \frac{5}{2}\underline{V}\rho\ T\Theta + \\ + \rho \underline{V}\varepsilon - \overline{K}_R\, T^3 \frac{\partial T}{\partial \underline{X}} \end{pmatrix} \right\rangle$$

$$= \left\langle \begin{pmatrix} 0 \\ 0 \\ \overline{P}_{fiss}\, \rho g(X) \end{pmatrix} \right\rangle \tag{4.6}$$

This equation, together with (2.16), can be used to generate equations for the averages $\langle\rho\rangle$, $\langle\underline{V}\rangle$, $\langle T\rangle$, etc., and fluctuations $\delta\rho$, $\delta\underline{V}$, δT, etc.

In the "stationary turbulence" state (and for one-dimension) it follows,

$$\langle \delta\rho\ \delta V \rangle = 0$$

$$\langle \rho \rangle \langle T \rangle \langle \theta \rangle + \langle \rho \rangle \langle \delta V^2 \rangle + \langle \delta\rho\ \delta T \rangle \langle \theta \rangle + \langle \delta T\ \sigma\theta \rangle \langle \rho \rangle$$

$$+ \langle \delta\rho\ \delta\theta \rangle \langle T \rangle + \langle \delta\rho\ \delta T\ \delta\theta \rangle = \langle P \rangle = \text{constant.}$$

$$\frac{\partial}{\partial X} \left\{ \frac{1}{2} \langle \delta\rho\ \delta V^3 \rangle + \frac{1}{2} \langle \rho \rangle \langle \delta V^3 \rangle + \frac{5}{2} \langle V\rho\ T\theta \rangle \right. \tag{4.7}$$

$$\left. + \langle \rho V\varepsilon \rangle - \bar{K}_R \langle T^3 \frac{\partial T}{\partial X} \rangle \right\} = \langle \bar{P}_{fiss}\ \rho g \rangle$$

We now see that the stationary solution to the above system differs from the stationary solution to (2.16) because of the various pressures, fluxes, etc., deriving from the fluctuations.

Returning to the exact system solved by computer, the fluid variables are expanded

$$\rho, V, T = \Sigma \left\{ (\rho_{sn}, V_{sn}, T_{sn}) \sin k_n x + (\rho_{cn}, V_{cn}, T_{cn}) \cos k_n x \right\} \tag{4.8}$$

where ρ_{oc}, V_{oc}, T_{oc} are functions of the "slow" time variable T and all other ρ_n, V_n, T_n are functions of both slow T and also oscillate on the fast t-scale. Also,

$$\langle \rho, V, T \rangle = (\rho_o, 0, T_o) \tag{4.9}$$

Pressure Fluctuations

Consider the fluctuating part of the pressure (including wave pressure),

$$\begin{aligned} \delta P &= P - \langle P \rangle \\ &= \rho V^2 + \rho T\Theta - \langle \rho T\Theta + \rho V^2 \rangle \\ &\equiv \sum_{n=1}^{\infty} \delta P_n \end{aligned} \tag{4.10}$$

The Fourier components δP_n all fluctuate about zero, as illustrated below:

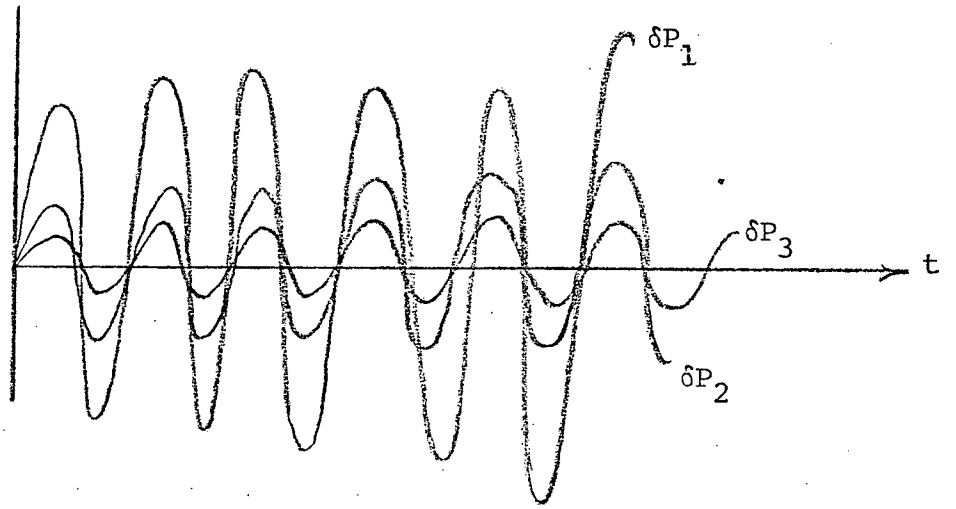

Figure 4.1

They are particularly simple to evaluate at the wall where V = 0 and $T = T_w$,

$$\delta P_w = T_w \Theta_w \sum_{n=1}^{\infty} \left\{ \rho_{ns} \sin k_n x + \rho_{nc} \cos k_n x \right\} \tag{4.11}$$

An alternate quantity of interest (which we will in fact plot using the computer results), is the total pressure fluctuation about the initial state, i.e.,

$$\widetilde{\delta P} = \rho V^2 + \rho T\Theta - (\rho T\,\Theta + \rho V^2)_{t=0} \tag{4.12}$$

In this case the various spatial Fourier components of $\widetilde{\delta P}$ oscillate in time about an average pressure that drifts away from the initial pressure due to the wave pressure terms, i.e., Fourier components appear as graphed below:

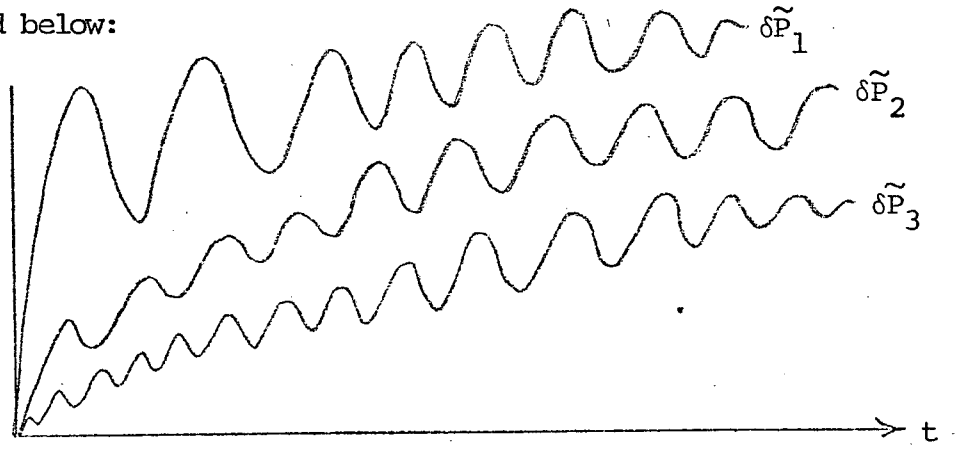

Figure 4.2

These are the quantities that will be plotted for various neutron gradients and reactor parameters in Figs. 4.2 - 4.7. They are graphed for the one-dimensional slab case. The asymptotic Fourier amplitudes are all about 1% for the cases considered with an enhancement of approximately a factor of 2 for the cases in which the neutron density gradient was nonuniform.

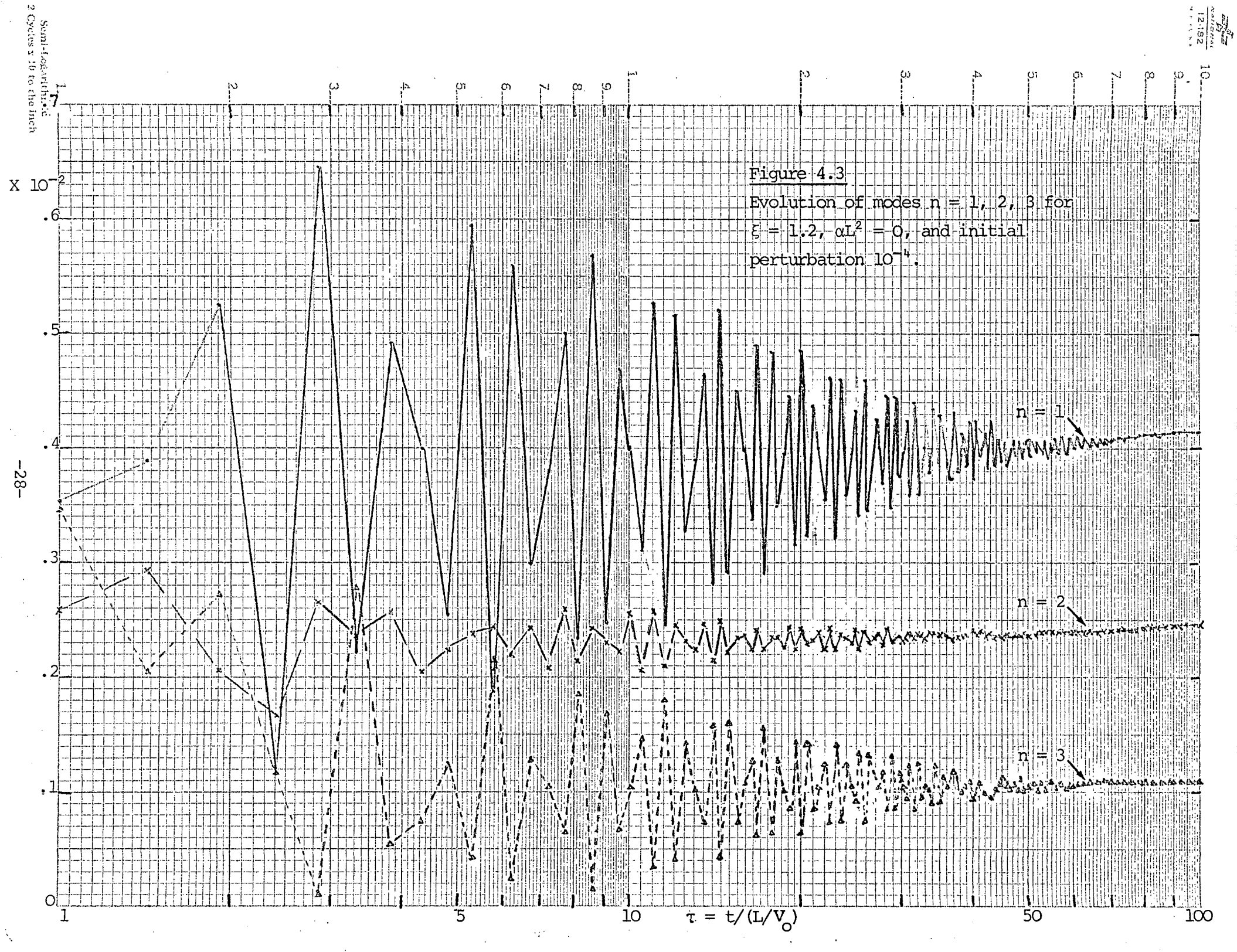

Figure 4.3
Evolution of modes n = 1, 2, 3 for $\xi = 1.2$, $\alpha L^2 = 0$, and initial perturbation 10^{-4}.

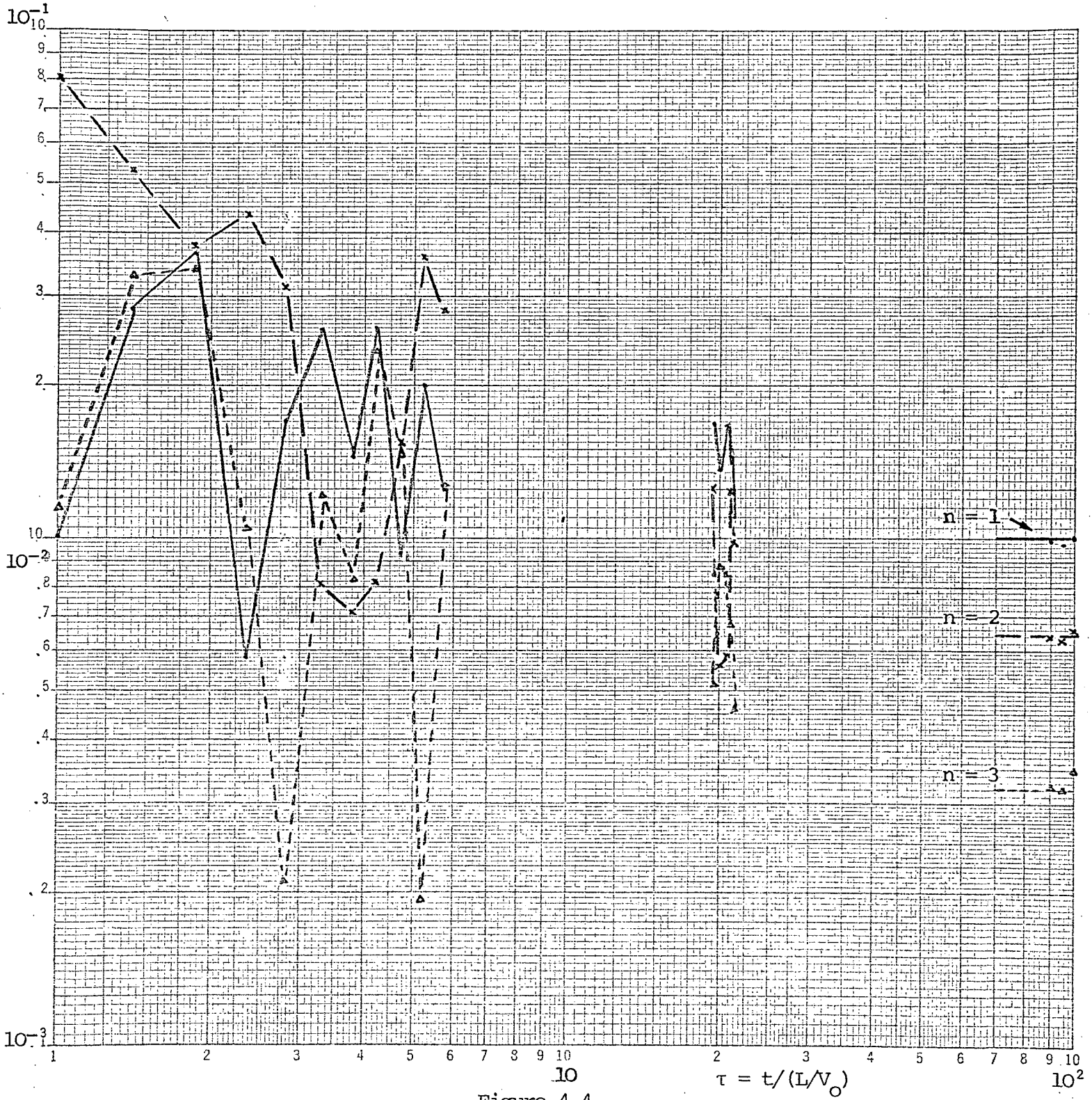

Figure 4.4

Evolution of modes n = 1,2,3 for $\xi = 1.4$, $\alpha L^2 = 0$.

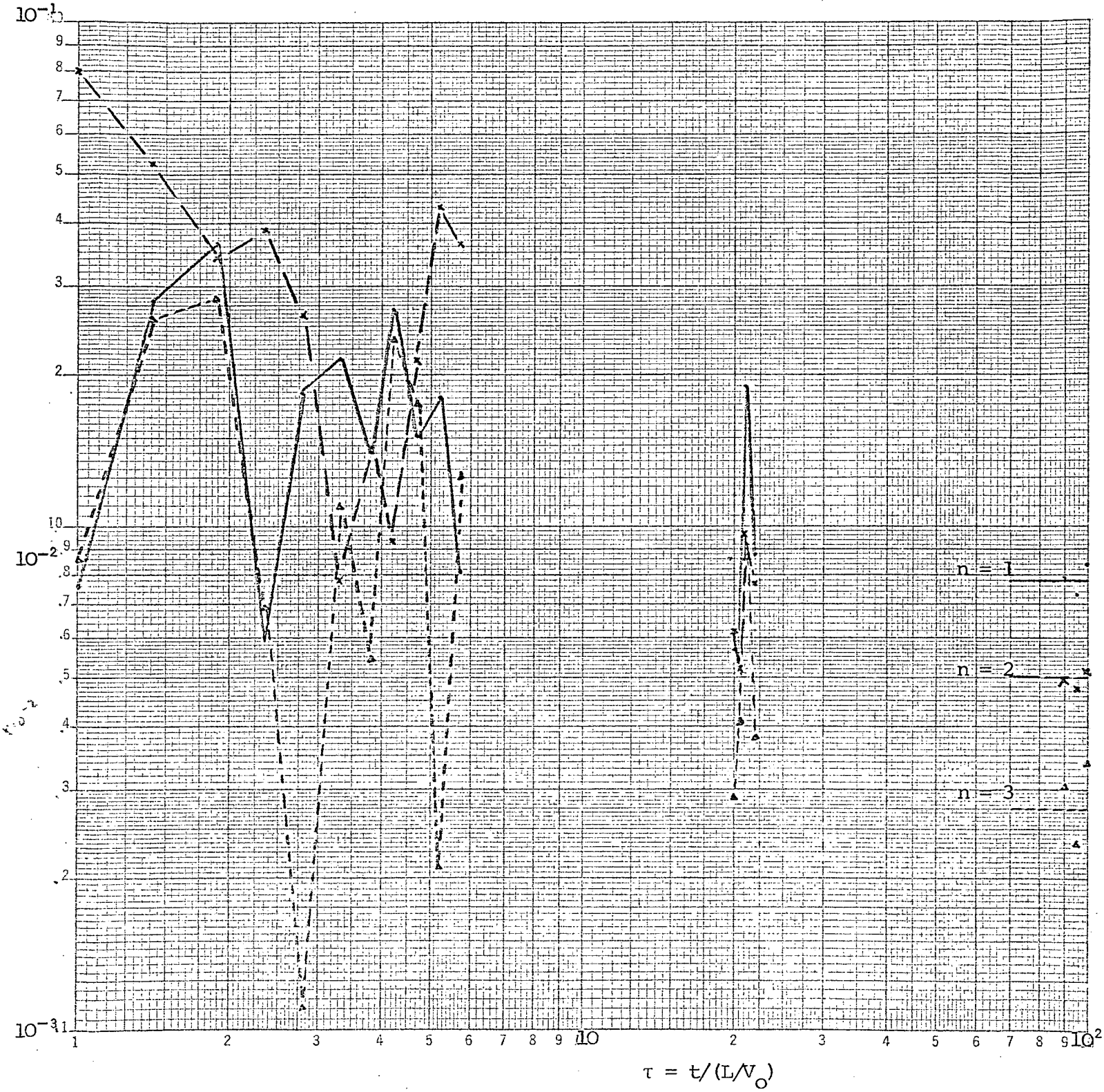

Figure 4.5

Evolution of modes n = 1, 2, 3 for $\xi = 1.2$, $\alpha L^2 = 2$.

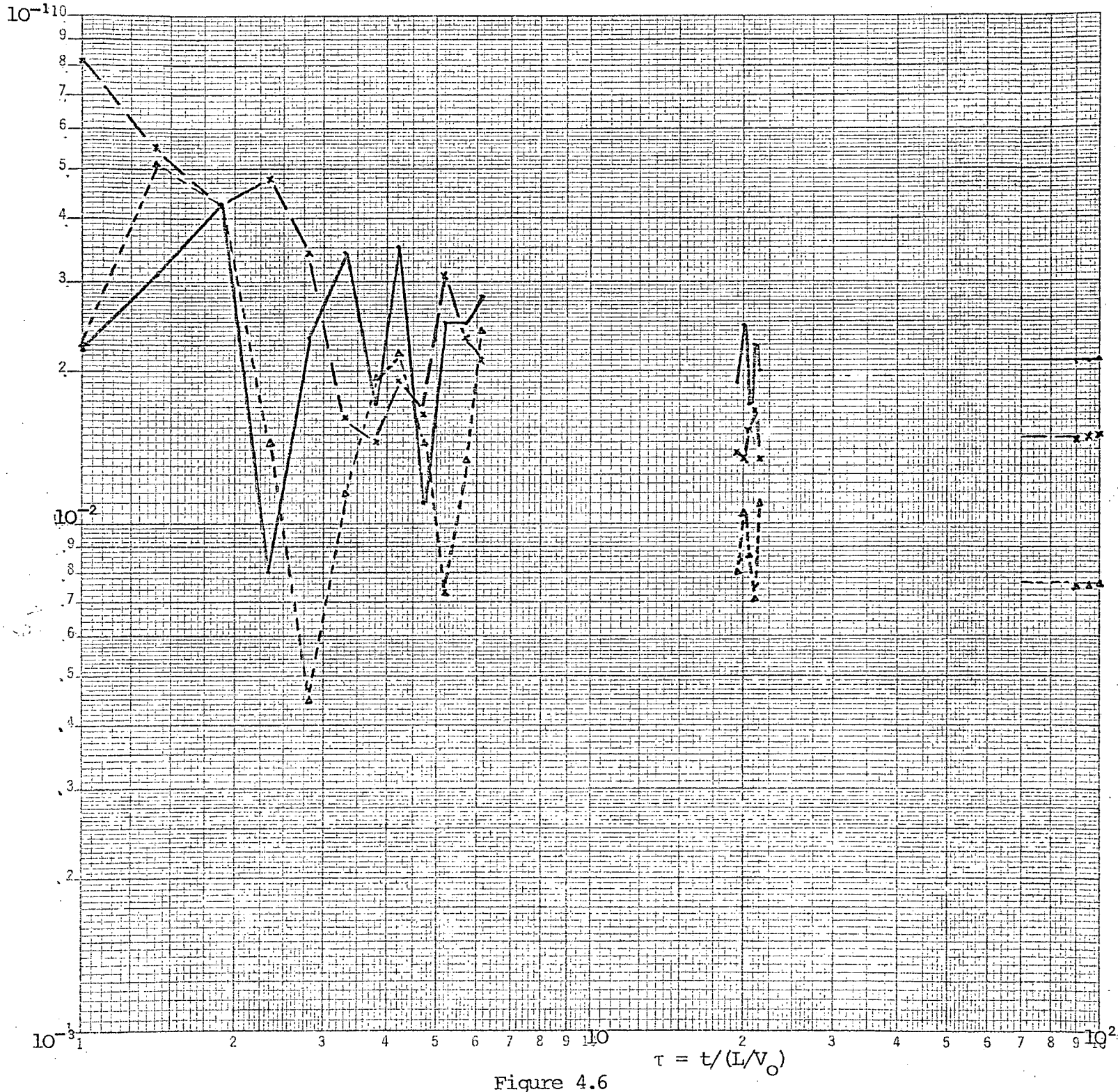

Figure 4.6
Evolution of modes n = 1,2,3 for $\xi = 1.4$, $\alpha L^2 = 2$.

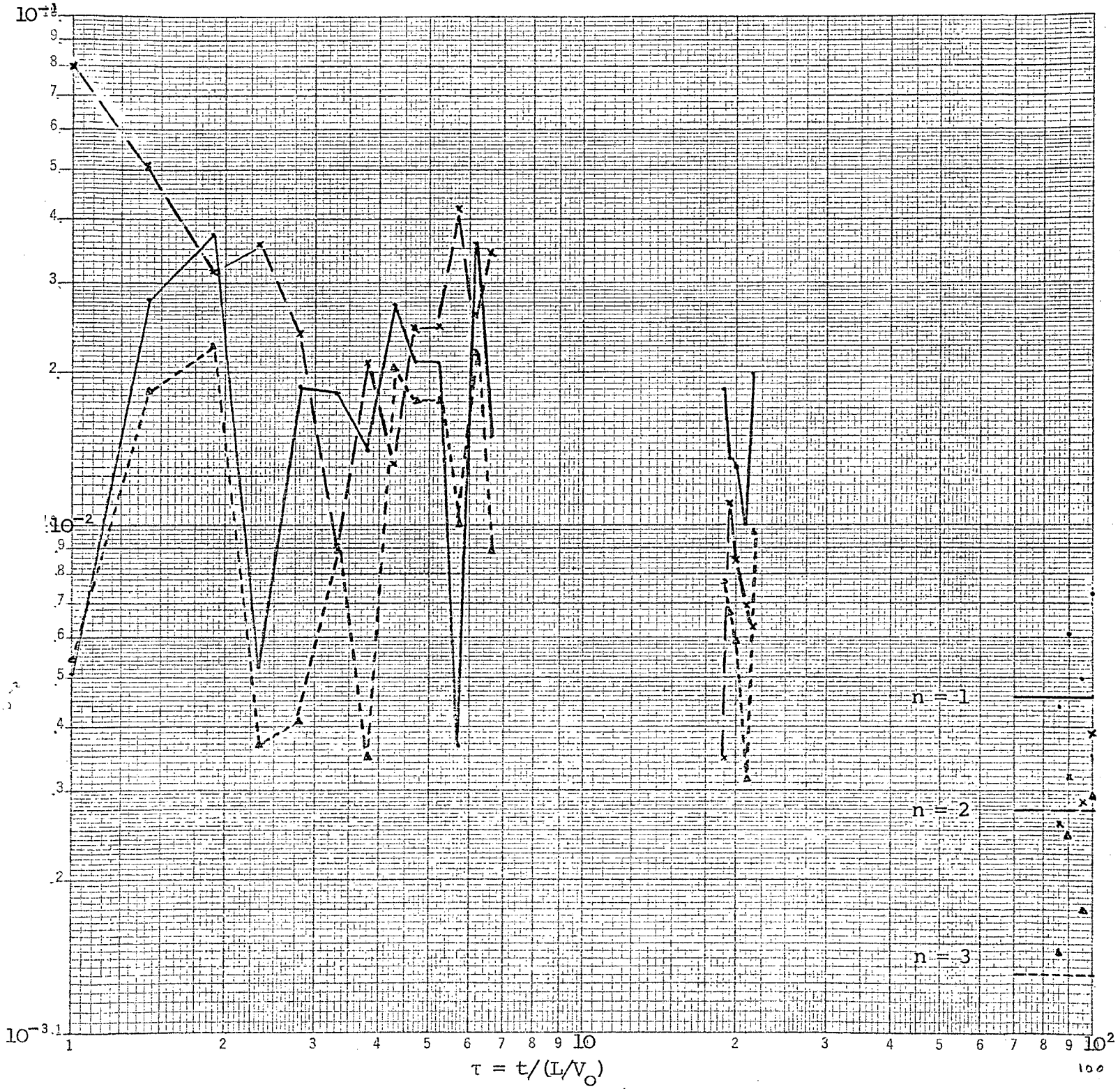

Figure 4.7
Evolution of modes n = 1,2,3 for $\xi = 1.2$, $\alpha L^2 = 0$.

Relation between Spherical and Slab Geometry for the Fissioning Plasma Problem

The equations for spherical or slab plasmas can be simply related.

Slab

$$\frac{\partial}{\partial \tau}\begin{pmatrix} \rho \\ \rho V \\ \frac{1}{2}\rho V^2 + \frac{3}{2}\rho T\Theta + \rho\varepsilon \end{pmatrix} + \frac{\partial}{\partial X}\begin{pmatrix} \rho V \\ \rho V^2 + \rho T\Theta \\ \frac{1}{2}\rho V^3 + \frac{5}{2} V\rho T\Theta + \rho V\varepsilon - \overline{K}_R T^3 \frac{\partial T}{\partial X} \end{pmatrix}$$

$$= \begin{pmatrix} 0 \\ 0 \\ \overline{P}_{fiss}\ \rho g \end{pmatrix} . \qquad (4.13)$$

Sphere

$$\frac{\partial}{\partial \tau}\begin{pmatrix} R^2\rho \\ \rho V \\ R^2[\ \frac{1}{2}\rho V^2 + \frac{3}{2}\rho T\Theta + \rho\varepsilon\ ] \end{pmatrix} + \frac{\partial}{\partial R}\begin{pmatrix} R^2\rho V \\ \rho V^2 + \rho T\Theta \\ R^2[\ \frac{1}{2}\rho V^3 + \frac{5}{2} V\rho T\Theta + \rho V\varepsilon - \overline{K}_R T\ \frac{\partial T}{\partial R}\ ] \end{pmatrix}$$

$$= \begin{pmatrix} 0 \\ 0 \\ R^2\overline{P}_{fiss}\ \rho g \end{pmatrix} \qquad (4.14)$$

where ρ, V, T, ε, $\overline{K}_R$, P_{fiss}, are the dimensionless density, fluid velocity, temperature, internal ionization energy, radiation diffusion coefficient,

and fission power density. The function g(X) is the neutron density in the cavity.

Now in (4.14) consider the variable change from R, V to X, W where

$$\begin{cases} X = \frac{4\pi}{3} R^3 \quad , \quad dX = 4\pi R^2 dR \\ W = 4\pi R^2 V \end{cases} \tag{4.15}$$

In terms of X, W, equation (4.14) becomes

$$\frac{\partial}{\partial \tau} \begin{pmatrix} \rho \\ \rho W \\ \frac{1}{2} \rho \left(\underline{\frac{W}{4\pi R^2}} \right)^2 + \frac{3}{2} \rho T\Theta + \rho\varepsilon \end{pmatrix} + \frac{\partial}{\partial X} \begin{pmatrix} \rho W \\ \rho \left(\underline{\frac{W}{4\pi R^2}} \right)^2 + \rho T\Theta \\ \rho W \left[\frac{1}{2} \left(\underline{\frac{W}{4\pi R^2}} \right)^2 + \frac{5}{2} T\Theta + \varepsilon \right] - \overline{K}_R T^3 \underline{(4\pi R^2)^2} \frac{\partial T}{\partial X} \end{pmatrix}$$

$$= \begin{pmatrix} 0 \\ 0 \\ \overline{P}_{fiss} \rho g \end{pmatrix} \tag{4.16}$$

This equation is now identical with (4.13) [where W now takes the place of V], except for the four underlined terms. Three of them replace occurrences of V^2 in the energy density with calculations from W; the fourth is a temperature difference in R instead of X. Thus, to solve the spherical problem with the slab solution one must make the replacements

where underlined. Note,

$$V \rightarrow \frac{W}{4\pi R^2} = \frac{W}{(4\pi)^{1/3}(3x)^{2/3}} \tag{4.17}$$

These relationships are useful in developing hydro-codes for the slab and sphere problems.

Comments on Radiation Flux Instabilities

It has been suggested that under some circumstances radiation flux may drive acoustic instabilities[17] in a U-plasma (see for example "An Acoustic Instability Driven by Absorption of Radiation in Gases" by M. J. Monsler, MIT Tech. Note CSRT-69-4 (1969)). Our set of equations (2.16) contains this physical possibility since a large radiation flux is of course present in the steady state reactor solution that is perturbed at $\tau = 0$.

It is fairly difficult to make a reliable analytic decision concerning this possibility, and Monsler's analysis had several weaknesses. However, in order to extract some limited information on this we considered a simple model for sound wave propagation in a medium that is treated as homogeneous except in terms involving the radiation flux. The linear equations are then

$$\frac{\partial N_1}{\partial t} + N_o \frac{\partial V_1}{\partial x} = 0 \tag{4.18}$$

$$\frac{\partial V_1}{\partial t} + \frac{K}{MN_o}\left(N_o \frac{\partial T_1}{\partial x} + T_o \frac{\partial N_1}{\partial x}\right) = 0 \tag{4.19}$$

$$\frac{3}{2}K\left(N_o\frac{\partial T_1}{\partial t}+T_o\frac{\partial N_1}{\partial t}\right)+\frac{5}{2}N_oKT_o\frac{\partial V_1}{\partial x}=\frac{\partial}{\partial x}\left(K_R\frac{\partial(T_o+T_1)}{\partial x}\right) \quad (4.20)$$

$$\simeq \alpha\frac{\partial T_1}{\partial x}+\beta T_1+K_R\frac{\partial^2 T_1}{\partial x^2} \quad .$$

It follows that modes $e^{i(\omega t-kx)}$ have a dispersion relation

$$\omega(3\omega^2-5k^2v^2)=-\frac{2i}{N_o}(\omega^2-k^2v^2)(-ik\alpha+\beta-K_Rk^2) \quad (4.21)$$

where $v^2 = KT_o/M$. Assuming radiation has a small effect one can write $\omega = \omega_o + \omega_1$ and treat ω_1 as small with $\omega_o = \sqrt{5/3}$ kv. This gives

$$\mathrm{Im}(\omega_1) = -\frac{2}{10N_o}(\beta-K_Rk^2) \quad .$$

The range of <u>stable</u> wavenumbers is

$$k^2 > k^2_{crit} = \frac{1}{K_R}\frac{\partial^2 K_R}{\partial T_o^2}\left(\frac{\partial T_o}{\partial x}\right)^2 \quad , \quad (4.22)$$

i.e.,

$$k_{crit} \simeq \frac{\sqrt{n(n-1)}}{\ell_T} \quad ,$$

where ℓ_T is the gradient scale of T_o and it has been assumed $K_R \alpha T^n$.

Now the approximations used in the analysis break down except for the wave number range k > several k_{crit}, i.e. (similar to a WKB assumption), short wavelength acoustic waves are <u>stable</u>. The analytic

question of the radiation stability of long wavelength waves with wavelengths $\sim \ell_T$ however remains open. Our computer studies bear out the conclusion that the radiation flux does not appear to give rise to instability.

5. STABILIZING EFFECT OF SOUND WAVE TRANSMISSION OUT OF THE REACTING PLASMA

Instability occurs because the average effect of P_{fiss} overcomes the damping effect of radiation diffusion for sound waves in the wavelength range $\lambda > \lambda_{crit}$. However, the growth rates are small (typically $10^{-2}\omega_R$), so that it is of interest to consider the damping effects due to escape of sound energy from the fissioning plasma.

In realistic situations sound wave energy is partially transmitted through the container walls (as well as down the orifice gas column in the rocket case). The question arises of how to represent this transmission coefficient in the equations.

Now the equations involve the fluxes $N_{u-u}V_{u-u}$ and energy flux $\underline{F}$. Obviously the wall boundary condition $N_{u-u}V_{u-u} = 0$ must not be changed since mass is conserved in the reactor even though energy is partially transmitted. The boundary condition representing transmission can most easily be introduced into the energy equation as a sink of sound energy density at the wall, i.e., rewrite the energy equation as

$$\frac{\partial E}{\partial t} + \underline{\nabla} \cdot \underline{F} = \underbrace{P_{fiss}}_{\text{(volume energy source)}} - \underbrace{S\,\delta(x - x_w)}_{\text{(wall sink)}} \tag{5.1}$$

where

$$E = \frac{1}{2} MN_u V_u^2 + \frac{3}{2} N_u KT_u (1 + Z) + N_u \mathcal{E} \tag{5.2}$$

$$\underline{F} = \underline{V}_u \frac{1}{2} MN_u V_u^2 + \frac{5}{2} \underline{V}_u N_u KT_u (1 + Z) + N_{u-u} V_{u-u} \mathcal{E} - K_R \underline{\nabla} T_u \tag{5.3}$$

and the wall is located at x_w.

Various models for S are possible. For example, a simple non-dispersive one is

$$S = \alpha|E_w(t) - E_o| \tag{5.4}$$

where E_o is the energy density for the stationary solution (taken as the zero-frequency part of E), and $E_w(t)$ the finite-frequency components of E evaluated at the wall. In this case if one considers the simple limit $P_{fiss} = 0$ and $K_R = 0$, (5.1) becomes

$$\frac{\partial E_w}{\partial t} = -\alpha|E_w - E_o| \quad \delta(x - x_w) \quad .$$

Since (as has already been assumed), E is nearly spatially homogeneous, an integration $\int_o^L dx$ removes the δ-function and gives

$$\frac{\partial E}{\partial t} = -\frac{\alpha}{L} (E - E_o) \quad . \tag{5.5}$$

Note the wall boundary conditions on which the code is based lets heat out of the system but not back in. Thus we consider only perturbations for which $E > E_o$. Equation (5.5) becomes

$$E - E_o = (E\ (t = 0) - E_o)e^{-\frac{\alpha t}{L}} \tag{5.6}$$

i.e., the system decays to its original stationary energy state E_o due to the escape of sound wave energy in a time L/α.

For the more general problem we will use (5.4) in equation (5.1). However it is useful to relate α to the transmission coefficient.

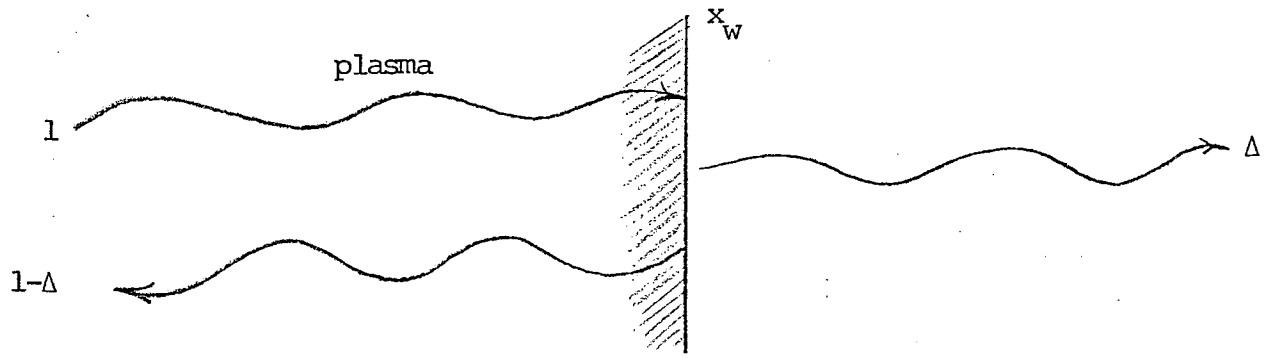

Figure 5.1

Assume a fraction Δ of the energy of a traveling sound wave is transmitted as shown, and that Δ is independent of frequency. In the perfectly reflecting case $\Delta = 0$, the standing wave solutions for the slab have amplitudes that vary in time only due to P_{fiss} and radiation diffusion. For $\Delta > 0$ however, their amplitude decreases due to escape of their decomposed traveling waves. The strength of the sink S in (5.1) can be written

$$S = \Delta \frac{1}{2} (E_w - E_o) V_s \tag{5.7}$$

where V_s is the sound speed at the wall and $(E_w - E_o)/2$ is the energy density in the right-traveling wave. Thus the exponential decay rate in (5.6) becomes

$$\exp \left[- \left(\frac{V_s \Delta}{2L} \right) t \right] .$$

Critical Transmission of Coefficient for Stability

Transmission of sound energy out of the reactor cavity will overcome its amplitude growth inside the cavity if

$$\frac{V_s \Delta}{2L} < \omega_I \quad , \tag{5.8}$$

where ω_I is the linear growth rate. This relation leads to a critical transmission coefficient such that if $\Delta > \Delta_{crit}$ the system is stable, i.e.,

$$\begin{aligned} \Delta > \Delta_{crit} &= \frac{2L\omega_I}{V_s} \qquad \text{(stable)} \\ \Delta < \Delta_{crit} &\qquad\qquad\quad \text{(unstable)} \end{aligned} \tag{5.9}$$

It should be pointed out that this relation is fairly accurate, but the exact computer solution with a generalized boundary condition allowing transmission will yield a more precise value for Δ_{crit}.

Now for reactors of interest, $\omega_I << \omega_R \simeq kV_s$, so that the appropriate growth rate calculated earlier is

$$\omega_I \simeq \frac{i(k_{crit}^2 - k^2)K_{Ro}\left[1 - \frac{KT_o}{MV_s^2}(1 + Z_o + N_o Z_N)\right]}{3N_o K\left[1 + Z_o + T_o Z_T + \frac{\mathcal{E}_T}{K}\right]} \tag{5.10}$$

Also, several modes are unstable with the fastest growing mode corresponding to k a minimum, i.e., we can write $k_{crit}^2 - k^2 \simeq k_{crit}^2$ and note

$$k^2_{crit} \simeq \frac{K(1 + Z_o + T_o Z_T) \left(\frac{P_{fiss,o}}{M} \right)}{K_{Ro} V_s^2 \left[1 - \frac{KT_o}{V_s^2 M} (1 + Z_o + N_o Z_N) \right]} \tag{5.11}$$

(Notation is as in our earlier report,[12] or the 1971 final report).

Thus

$$\omega_I = \frac{\eta P_{fiss,o}}{3MN_o V_s^2} \tag{5.12}$$

with

$$\eta = \left(\frac{1 + Z_o + T_o \epsilon_T}{1 + Z_o + T_o Z_T + \frac{\epsilon_T}{K}} \right) \simeq 1 \quad .$$

It follows that

$$\Delta_{crit} = \left(\frac{L}{V_s} \right) \eta \left(\frac{P_{fiss,o}}{3MN_o V_s^2} \right)$$

or, since $\omega_R = kV_s = \pi V_s / L$ (for the slab),

$$\Delta_{crit} = \pi \left(\frac{\omega_I}{\omega_R} \right) = \eta \pi \frac{1}{\omega_R} \left(\frac{P_{fiss,o}}{3MN_o V_s^2} \right) \quad . \tag{5.13}$$

Typical values are

$$\begin{cases} P_{fiss,o} = 1.3 \cdot 10^{10} \text{ ergs/cm}^3\text{/sec} \\ MN_o = 6 \cdot 10^{-3} \text{ gm/cm}^3 \\ V_s = 2.7 \cdot 10^5 \text{ cm/sec} \\ L \simeq 10^2 \text{ cm} \end{cases}$$

so that $\Delta_{crit} \simeq 4 \cdot 10^{-3}$.

For example, consider the open cycle reactor in which waves are trapped in the cavity except when traveling out the nozzle as shown. An approximate effective transmission coefficient is

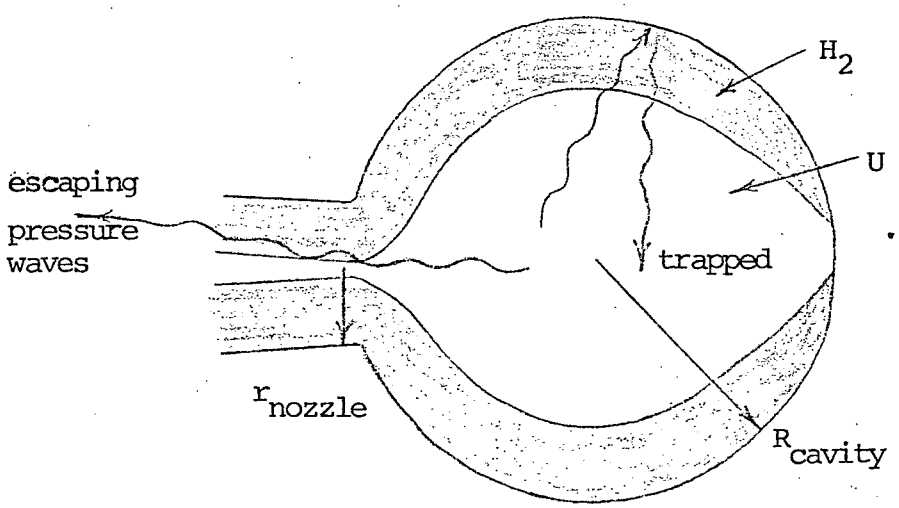

$$\Delta_{effective} = \frac{r^2_{nozzle}}{4\, R^2_{cavity}} \tag{5.14}$$

Figure 5.2

i.e., we would expect the escape of sound wave energy to stabilize the acoustic mode provided $\Delta_{crit} < \Delta_{effective}$, i.e., $r_{nozzle} > .13\, R_{cavity}$.

REFERENCES

There is an extensive literature on studies of gas-cored nuclear reactors. The first five papers cited below contain useful lists of references.

1. F. E. Rom, Comments on the feasibility of developing gas core nuclear reactors, Lewis Research Center NASA Tech. Note TMX-52644(1969). This contains 78 references with titles:

   See also:

   R. W. Bussard and R. D. DeLauer, Fundamentals of Nuclear Flight, McGraw-Hill Book Company, Inc., New York, 1965

   and

   R. G. Ragsdale, Relationship Between Engine Parameters and Fuel Mass Contained in an Open-Cycle Gas-Core Reactor, Report NASA-TM-X-52733, National Aeronautics and Space Administration, January 1970.

2. Research on Uranium Plasmas and their Technology Applications, Proceedings of NASA-sponsored symposium at University of Florida, January 1970, edited by Karlheinz Thom and Richard T. Schneider.

3. Second Symposium on Uranium Plasmas: Research and Applications, November 1971. Published by American Inst. of Aeronautics and Astronautics, 1290 Sixth Ave., New York, New York 10019.

4. H. F. Atwater, H. E. Wilhelm, and R. B. Perez, Theoretical Investigation of a Self-Sustained Nuclear Plasma Source, Report to NASA under Grand NGR10-005-068 from Dept. of Nucl. Eng., University of Florida, 1968.

   This contains a list of 75 references with titles, and also many useful calculations for uranium plasmas.

5. A useful recent review, also containing many references, is entitled "Gas-Core Reactor Technology" by J. D. Clement and J. R. Williams, in Reactor Technology 13, 226 (1970).

6. See for example J. R. Williams, Proc. 2nd Symposium on Uranium Plasmas: Research and Applications, page 65, Nov. 1971, and other papers in this volume.

7. R. J. Rosa, Magnetohydrodynamic Energy Conversion, McGraw-Hill Book Company, Inc., New York, 1968.

8. A. Sherman, Gaseous Fission Closed Loop MHD Generator, in Proceedings of the Symposium on Research on Uranium Plasmas and Their Technological Applications, University of Florida, January 1970.

9. R. J. Rosa, Propulsion System Using a Cavity Reactor and Magneto-hydrodynamic Generator, Amer. Rocket Soc. J., July 1961.

10. J. R. Williams and S. V. Shelton, Gas-Core Reactors for MHD Power Systems, in Proceedings of the Symposium on Research on Uranium Plasmas and Their Technological Applications, University of Florida, January 1970.

11. See papers in References 2 and 3.

12. See page 99 of Reference 3, and "Instabilities in Uranium Plasma and the Gas-Core Nuclear Rocket Engine," D. A. Tidman (Final report to NASA, May 1972, contract NASW-2231).

13. L. V. Gurvich and V. S. Yugman, Calculation of the Thermodynamic Properties of Gaseous Uranium and Plutonium and Their Ions Up to 20,000°K, in Thermodynamics with Emphasis on Nuclear Materials and Atomic Transport in Solids, Vol. 2, p. 613, International Atomic Energy Agency, Vienna, 1966.

14. A. S. Keston and N. L. Krascella. Theoretical Investigation of Radiant Heat Transfer in the Fuel Region of a Gaseous Nuclear Rocket Engine, Report NASA-CR-695, United Aircraft Corporation, January 1967.

15. D. E. Parks, G. Lane, J. C. Stewart, and S. Peyton, Optical Constants of Uranium Plasma, Report GA-8244 (NASA-CR-72348), Gulf General Atomic Incorporated, February 1968.

16. R. W. Patch, Status of Opacity Calculations for Application to Uranium-Fueled Gas-Core Reactors, Report NASA-TM-X-52722, January 1970.

17. M. J. Monsler, MIT Tech. Note CSRT-69-4 (1969).